Compensation strategy of shoulder synergist muscles is not stereotypical in patients with rotator cuff repair

Jun Umehara, PhD,[1,2] Masahide Yagi, PhD,[1] Yasuyuki Ueda, PhD,[1,3] Shusuke Nojiri, MSc,[1] Kotono Kobayashi, MSc,[1] Takashi Tachibana, BS,[4] Katsuya Nobuhara, PhD,[5] Noriaki Ichihashi, PhD[1]

[1] Human Health Sciences, Graduate School of Medicine, Kyoto University, Kyoto, Japan

[2] Faculty of Rehabilitation, Kansai Medical University, Osaka, Japan

[3] Faculty of Health Science, Takarazuka University of Medical and Healthcare, Takarazuka, Japan

[4] Department of Rehabilitation, Nobuhara Hospital, Tatsuno, Japan

[5] Institute of Biomechanics, Nobuhara Hospital, Tatsuno, Japan

Corresponding author:

Jun Umehara, PhD

Human Health Sciences, Graduate School of Medicine, Kyoto University

53 Kawahara-cho, Shogoin, Sakyo-ku, Kyoto 606-8507, Japan

Phone: +81-90-4767-5013

E-mail: umehara.jun.77z@st.kyoto-u.ac.jp

Running title:

Compensation after rotator cuff repair

Word count:

Abstract: 244/250

Main text: 4200/4200

Author Contributions Statement:

All authors have made substantial contribution to the research designe, or the acquisition, analysis or interpretation of data. All authors drafted or revised the manuscript critically. All authors approved the final manuscript.

Abstract

Rotator cuff tear is a common shoulder injury that causes shoulder dysfunction and pain. Although surgical repair is the primary treatment for rotator cuff tear, it is well recognized that impaired force exertion of muscles connecting to the involved tendon and subsequent complemental change in the force exertion of synergist muscles persist even after repair. This study aimed to identify the compensation strategy of shoulder abductors by examining how synergist muscles respond to supraspinatus muscle force deficit in patients with rotator cuff repair. Muscle shear modulus, an index of muscle force, was assessed for supraspinatus, infraspinatus, upper trapezius, and middle deltoid muscles in repaired and contralateral control shoulders of 15 patients with unilateral tendon repair of the supraspinatus muscle using ultrasound shear wave elastography while the patients passively or actively held their arm in shoulder abduction. In the repaired shoulder, the shear modulus of the supraspinatus muscle declined, whereas that of other synergist muscles did not differ relative to that of the control. To find the association between the affected supraspinatus and each of the synergist muscles, a regression analysis was used to assess the shear moduli at the population level. However, no association was observed between them. At the individual level, there was a tendency of variation among patients with regard to a specific muscle whose shear modulus complementarily increased. These results suggest that the compensation strategy for supraspinatus muscle force deficit varies among individuals, being non-stereotypical in patients with rotator cuff injury.

Keywords

elastography; compensation; shear modulus; muscle force; rotator cuff

Introduction

Rotator cuff tear is a common shoulder injury that causes dysfunction and pain in the shoulder joint. The prevalence of rotator cuff tear increases with aging,[1] occurring in more than 40% of the population above the age of 60 years.[2; 3] Surgical repair of the involved tendon is a common primary treatment for rotator cuff tear.[4] However, it is well recognized that impaired force exertion of the muscle connecting to the involved tendon persists even after repair. Additionally, synergist muscles undergo complementary changes owing to impaired force exertion.[5-7] Specifically, since the supraspinatus (SSP) muscle, one of the rotator cuff muscles, is most susceptible to tendon tear,[8; 9] the deficit in SSP muscle force and the subsequent complementary change in the force exertion of synergist muscles (e.g., deltoid, upper trapezius, and remaining rotator cuff muscles) seem to be prominent in clinical settings.

Such complementary changes in synergist muscle behavior following agonist muscle contribution deficit are generally known as compensation strategies. To date, several methods have been proposed to investigate compensation strategies in shoulder muscles. For instance, electromyography has been used for patients after rotator cuff repair; however, the crucial activity of the SSP muscle cannot be measured directly due to its location beneath the upper trapezius muscle.[10] Nevertheless, using a needle/wire electrode could enable SSP muscle activity to be recorded,[11; 12] but the normalization procedure and pain induced by needle/wire insertion could under- or overestimate the inherent capacity of the muscle. Biomechanical studies using cadavers have been used to investigate the effect of SSP tendon tear on other muscles.[13-15] However, these studies only clarified the mechanical effects and were not able to investigate the pain-induced changes in motor command sent to the muscles. A recent study attempted to identify the compensation strategy using a computational musculoskeletal model.[16; 17] However, since this model was not developed as a subject-specific model for patients with rotator cuff repair, it could not represent the inherent neuromuscular capacity of patients.

Currently, ultrasound shear wave elastography (SWE) is a promising technology for studying muscle mechanics. SWE can non-invasively quantify the muscle shear modulus,[18] an index of individual muscle force during active contraction.[19; 20] A few studies utilized SWE to examine the elasticity of the SSP muscle in patients with rotator cuff tear[21] and repair[22] but did not measure other synergist muscles. Although a recent study investigated synergist muscles in addition to the SSP muscle in patients with rotator cuff repair,[23] it did not focus on the compensation strategy between them.

In summary, no studies have investigated the complementary relationship between the SSP muscle and other synergist muscles in patients. Therefore, using SWE, this study aimed to identify the compensation strategy of shoulder abductors by examining how synergist muscles behave following force decline in the SSP muscle in patients with rotator cuff repair. We hypothesized that the middle deltoid muscle acts in a compensatory manner with regard to the SSP muscle, based on previous studies using cadavers[13-15] and musculoskeletal models.[16; 17]

Methods

1. Participants

Thirty-six patients who underwent unilateral rotator cuff repair between June 2019 and December 2020 using the McLaughlin procedure, an open surgical approach, were recruited from an orthopedic hospital to participate in this study. The inclusion criteria for the repaired shoulder were as follows: (i) postoperative period from 8 weeks to 1 year, (ii) supraspinatus tendon solo tear, (iii) small to medium tear before surgery, (iv) no retear, and (v) more than 90° abduction. The inclusion criteria for the contralateral control shoulder were as follows: (i) no symptoms, (ii) no history of any orthopedic disease or surgery, and (iii) no current tear. Retear in the repaired shoulder and asymptomatic tear in the control were sonographically diagnosed by two examiners (J.U. and Y.U.) based on the criteria, and discontinuity, thinning, hypoechogenicity, and irregularity were judged as tears.[24] Following these norms, 10 patients who did not meet the criteria for repaired shoulders and 6 who did not meet the criteria for control shoulders were excluded. Additionally, five patients were excluded due to problems associated with ultrasound measurement and processing. Specifically, four were excluded owing to an identified non-trivial muscle contraction during the elastography measurements, and one was excluded owing to the several voids within the colormap under the elastographic image analysis. Consequently, data for 15 patients (age 64 ± 9 years, height 164 ± 8 cm; body mass, 66 ± 10 kg, 10 males) were analyzed in this study. The shoulder characteristics, functions, and symptoms of patients are presented in Table 1. The study protocol was approved by the Ethics Committee of Kyoto University Graduate School and the Faculty of Medicine (R1277) and the Institutional Review Board of Nobuhara Hospital and Institute of Biomechanics (no. 188). In addition, we explained the aim and procedures of the study to all the participants and obtained written informed consent.

2. Protocol

This study was designed as a cross-sectional case-control study. Ultrasound assessments were conducted in the repaired and contralateral control shoulders by two examiners (J.U. for elastography and M.Y. for B-mode). In the ultrasound assessment, elastographic images were acquired from the SSP, infraspinatus (ISP), upper trapezius (UT), and middle deltoid (MD) muscles of the repaired and control shoulders in abduction tasks. We selected these muscles because of their roles as capital shoulder abductors.[25] Additionally, B-mode images were also acquired to assess muscle size and intramuscular fat, considering that these factors could influence the elastographic assessment of the muscle.[26-29]

3. Ultrasound measurement

3.1. Shear wave elastography

Muscle shear modulus was measured via elastography during abduction tasks. The shear modulus can be used as an index of individual muscle force because it reportedly increases linearly with joint torque primarily generated by one muscle crossing a joint (i.e., the joint torque is approximately equal to the individual muscle force).[19; 20] We used a previously described measurement posture.[21; 23; 30] Briefly, while seated on stools, the patients passively or actively held their arms at 30° of shoulder abduction (Figure 1A and B). We selected this posture as previous studies have demonstrated that it is associated with high activation[31] and large moment arm of the SSP muscle,[25] causing it to contribute to shoulder abduction torque. In other words, this measurement posture should impose synergist muscles to contribute to torque exertion when SSP muscle force declines.

In the passive and active abductions, the shear moduli of the SSP, ISP, UT, and MD muscles were measured using an ultrasound system (Aixplorer v12.2; Hologic Supersonic Imagine, Aix-en-Provence, France) coupled with a linear transducer (2–10 MHz, SuperLiner SL10-2; Hologic Supersonic Imagine) in the SWE mode (mode: MSK muscle, opt: penetration, frequency: 1.7 Hz, smoothing level: five, persistence: off, opacity: 100%, gain: 90%, colormap scale: 0–300 kPa). Before image acquisition, the measurement site of each muscle was marked on the skin. The measurement sites included the middle of the line between the half point of the scapular spine and that of the clavicle for the SSP muscle; the intersection of the line between the half point of the scapular spine and the inferior angle and line between the half point of the scapular medial border and greater tubercle of the humerus for the ISP muscle; middle of the seventh cervical vertebra and scapular acromion for the UT muscle; middle of the scapular acromion and deltoid tuberosity for the MD muscle. Owing to mechanical and functional significance, the posterior deep region and the middle portion were selected as the measurement regions for SSP and ISP, respectively.[32; 33]

For elastographic imaging, the probe was transversely placed on the muscle belly and then rotated parallel to the muscle fascicles by clearly identifying muscle fascicles on the B-mode image. The elastography region of interest (ROI; 10 mm × 10 mm) was set at similar locations across patients at approximately 2.5, 1.5, 1.0, and 1.5 cm below the skin for the SSP, ISP, UT, and MD muscles, respectively. Three consecutive images of each muscle were acquired during the steady state of the color map by a single probe positioning under careful monitoring. This consecutive image acquisition was conducted considering the possibility of muscle fatigue during active abduction. Image acquisition was conducted in the passive condition, followed by the active condition.

3.2. B-mode

Muscle size and intermuscular fat were investigated using B-mode ultrasound. The patients were seated on stools in a natural posture (Figure 1C). B-mode images were acquired for SSP, ISP, UT, and MD muscles using an ultrasound system (Noblus; Hitachi Aloka Medical Systems, Tokyo, Japan) with a linear transducer (L64, 5–18 MHz). The measurement parameters were set as a gain of 25 dB, dynamic range of 70, depth of 4.0 cm, and the shallowest focus across all patients. The measurement site of each muscle was the same as that in the elastography measurement. The probe was transversely placed on the measurement site to the muscle path, and two images were obtained from each muscle upon muscle fascicle visualization. We repeatedly removed the probe from the shoulder to acquire the images.

4. Image processing

4.1. Elastographic image

The muscle shear modulus was calculated from the elastographic image. The elastographic images were processed using the Aixplorer software built into the ultrasound system. A circular Q-box with a 10 mm diameter was set in the center of the ROI of each image (Figure 1A and B). The size of the Q-box was reduced to accommodate only the muscle in cases of decreased muscle thickness. Next, the mean value of the shear modulus within the Q-box was calculated. The shear modulus was averaged across three images of each muscle and then used for the statistical analysis. Note that the software calculated Young's modulus (E) by multiplying the shear modulus (G) by the constant of 3 but this constant is incorrect due to the muscle's anisotropic property. Therefore, we divided Young's modulus by 3 to reverse the software's calculation and obtain the accurate value of shear modulus that is equal to a square of shear wave velocity (Vs^2) multiplied by muscle density (ρ) (i.e., $E \cong 3G = 3\rho Vs^2$, where ρ is assumed as 1.0 g/cm^3).[34] The intra-observer reliability for the muscle shear modulus is presented in Table 2 as the intraclass correlation coefficient (ICC) using the model of case 1.

4.2. B-mode image

The muscle thickness and echo intensity were calculated from B-mode images. The echo intensity fairly reflects the intramuscular fat, as shown by comparison with magnetic resonance immaging[35] and computed tomography.[36] These measures were used to quantify muscle size and intermuscular fat, as previously reported.[37,38] The B-mode images were exported from the ultrasound system to a personal computer as tagged image format files and processed using the ImageJ software (National Institutes of Health, Bethesda, MD, USA). For muscle thickness, the distance between the upper and lower fasciae or between the fascia and bone was measured at the center of each measured image. For echo intensity, the mean value of all pixel intensities within the ROI was calculated from each measured image scaled from 0 (black) to 255 (white). The ROI was formed as a rectangular box and set to include as much muscle as possible while avoiding muscle fasciae and the bone (Figure 1C). The intra-observer reliabilities for muscle thickness and echo intensity are presented in Table 2 as ICCs using the model of case 1.

5. Statistics

All statistical analyses were performed in Matlab R2019b (MathWorks, Natick, MA, USA) and Spyder version 5 (Python 3.8.12) on Anaconda 4.10.3 (Anaconda, Austin, TX, USA). Data normality was assessed using a Shapiro–Wilk test. The shoulder range of motions, muscle thickness, and echo intensity were compared between repaired and control shoulders using Welch's *t*-test. When normality was violated, a Mann–Whitney U test was alternatively used.

We used a linear mixed-effects (LME) model to evaluate the difference in shear modulus of the SSP muscle and complementary changes in synergists such as UT, ISP, and MD muscles in the repaired shoulder. This model specified *shoulder side* (repaired and control), *contraction condition* (passive and active), and their interaction as fixed effects, the individual shoulder as a random effect, and the shear modulus of each muscle as the dependent variable. Additionally, to ensure whether the total amount of force exerted by SSP and synergist muscles are equivalent between repaired and control shoulders, the pooled active shear modulus of all muscles was compared between repaired and control shoulders using the LME model. Moreover, since muscle size and intramuscular fat could influence the shear modulus,[26; 28; 29] another LME model was constructed by adding muscle thickness and echo intensity as covariates to eliminate potential biases in determining the shear modulus. An analysis of variance (ANOVA) was used to test model significance, and the Tukey HSD post-hoc test was performed when significant main effects were observed.

To analyze the compensation strategy, we performed population- and individual-level analyses. For the population-level analysis, a simple linear regression analysis was used to determine associations between the SSP and each synergist muscle in the repaired shoulder. The dependent and independent variables were the active shear moduli of the SSP and those of each synergist muscle, respectively. For the individual-level analysis, the ratio of the active shear modulus of the repaired shoulder relative to that of the control was calculated for each muscle. A ratio > 1 suggested that the given muscle exerted more force than that of the control shoulder and complementarily contributed to force exertion. Subsequently, the patients were categorized into subgroups based on the highest ratio to identify the synergist muscle that executed the abduction task. Specific patterns in subgroups were observed in terms of pain, the Western Ontario Rotator Cuff (WORC) score, and postoperative day. The level of significance was set at $p < 0.05$.

Results

1. Patient characteristics

The shoulder characteristics, functions, and symptoms are presented in Table 1. All range of motions of the repaired shoulder were significantly reduced relative to those of the control shoulder. Sixty percent of the repaired shoulder was the dominant limb. The muscle thickness and echo intensity are shown in Table 3. Neither the muscle thicknesses nor the echo intensities of all muscles differed between repaired and control shoulders, except for the significantly higher echo intensity of the MD muscle.

2. Shear modulus of shoulder abductors

The shear modulus of each muscle during passive and active conditions is shown in Figure 2, and all statistical values of ANOVAs are listed in Table 4.

Regarding the SSP muscle, the LME models revealed no significant interaction between *shoulder side* and *contraction condition* and significant main effects of *shoulder side* and *contraction condition*. The shear modulus was significantly increased in the active condition compared with that in the passive condition ($p < 0.001$, $d = 3.27$). With regard to *shoulder side*, the shear modulus was significantly lower in the repaired shoulder than in the control shoulder ($p = 0.004$, $d = 1.16$). The LME model with covariates also revealed no significant interaction between *shoulder side* and *contraction condition* and significant main effects of *shoulder side* and *contraction condition*. These results indicated that the shear modulus of the SSP muscle increased during active abduction but decreased in the repaired shoulder and was unaffected by muscle thickness and echo intensity.

For synergist muscles, the LME models indicated that the shear moduli of UT, ISP, and MD muscles significantly varied depending on *contraction condition*, increasing during active abduction (UT: $p < 0.001$, $d = 2.94$; ISP: $p < 0.001$, $d = 2.13$; MD: $p < 0.001$, $d = 4.01$). However, the interaction and *shoulder side* main effects were not significant. The inclusion of muscle thickness and echo intensity as covariates did not alter the interaction and main effects of *shoulder side* and *contraction condition*.

Considering the decrease in the shear modulus of the SSP muscle, combined with unaltered synergist muscles during active abduction, an overall reduced shear modulus of all muscles was expectable in the repaired shoulder. Notably, however, the LME did not indicate significant effects of the *shoulder side*, indicating that the pooled active shear moduli of all muscles did not vary between repaired and control shoulders. Furthermore, the inclusion of muscle thickness and echo intensity as covariates did not alter the results.

3. Compensation strategy among synergist muscles

The population-level linear regression analysis to determine the compensation strategy among synergist muscles did not reveal any significant predictor variables; therefore, none of the synergist muscles could explain the active shear modulus of the SSP muscle (UT: $R^2 = 0.01$, $p = 0.707$; ISP: $R^2 = 0.01$, $p = 0.673$; MD: $R^2 = 0.06$, $p = 0.387$) (Figure 3).

The ratio of active shear modulus between the repaired and control shoulders at the individual level is shown in Figure 4A. The ratio of the SSP muscle was < 1 in almost all patients, whereas that of at least one synergist muscle was > 1 in all patients, except for two (patients #8 and #13). The order of the ratios among all muscles is shown in Figure 4B. The patients were categorized into three groups based on the highest ratios; three, five, and seven patients presented the highest ratios for UT, ISP, and MD muscles, respectively. These results indicate that the specific muscle acting to compensate for the decrease in the shear modulus of SSP muscle varies among patients. Moreover, pain, the WORC score, and postoperative day were subjectively compared among the subgroups (Figure 4C). The patients with the highest ISP muscle ratio might experience slight shoulder pain and have a bipolarized WORC score, whereas those with the highest MD muscle ratio might present with light or severe shoulder pain and high or low WORC scores.

Discussion

This study aimed to identify the compensation strategy of shoulder abductors in patients with supraspinatus tendon repair. We hypothesized that the MD muscle acts complementarily to the SSP muscle. Contrary to our hypothesis, we found no complementary relationship between SSP and MD muscles nor any synergist muscle complementarity at the population level. However, the specific muscles acting to compensate for the force deficit in the SSP muscle varied among the patients at the individual level. These results suggest a variable non-stereotypical compensation strategy among patients with rotator cuff repair.

Previous studies have used cadavers and computational models to determine the compensation strategy following rotator cuff tear and repair.[13-16] Our findings are inconsistent with those of previous studies that showed specific muscle(s) working in a compensatory role. Cadaveric studies have been used to investigate the influence of supraspinatus tendon tear and its repair on other shoulder muscles;[13-15] they found that the deltoid muscle acts complementarily in abduction movement. In addition, a computational study simulated the alteration of shoulder muscle force distribution after rotator cuff tear by modeling attenuated supraspinatus muscle force and observed compensation by the remaining rotator cuff and surrounding intact muscles (e.g., middle and posterior deltoid and latissimus dorsi) for the loss of muscle force to maintain joint mechanical integrity.[16] These studies provided quantitative evidence for the compensation strategy; however, the methodological approaches (e.g., cadavers and nominal musculoskeletal models) used in these studies do not truly reflect the conditions in a living patient. Thus, the inconsistencies between these studies and our results could be attributed to the methodological differences.

Our results are counterintuitive in light of the optimal control theory, which states that behaviors are achieved by minimizing the cost function.[39] In the present study, the cost function would be muscle force or activity. Considering the muscle moment arm and physiological cross-sectional area that determine force generation, the shear modulus of the MD muscle may theoretically increase because both its moment arm and physiological cross-sectional area could be greater than those of other synergist muscles,[25; 40] although the present results do not provide strong support for this possibility because the moment arm and physiological cross-sectional area could not be assessed in this study. However, while some patients exhibited increased MD muscle shear modulus, others showed increase in the shear moduli of ISP and UT muscles. Although shoulder pain and the WORC score were slightly associated with favorably increased muscle shear moduli, patient characteristics could not fully explain the results. One possible factor in determining the compensatory strategy is the heuristics of individual patients, since there may be no rules determining specific compensatory muscles, which could vary in individual patients. In this context, we demonstrated that muscle coordination is habitual rather than optimal when one agonist muscle force is lost.[41] Empirical research has also reported that induced acute back pain leads to non-stereotypical but variant muscle activation patterns among participants.[42] Therefore, the inconsistent changes in muscle shear modulus at the population level may be attributed to the heuristics of individual patients.

Our results are consistent with those of previous studies that used elastography to investigate the mechanical properties of muscles during contraction following rotator cuff repair. For the SSP muscle, Sakaki, et al. [23] reported that the shear modulus of the anterior deep region was lower in the repaired shoulder than in the contralateral unaffected shoulder during contraction 6 months post-surgery, although a regional difference in shear modulus change was observed. Furthermore, Ishikawa, et al. [43] reported that the muscle strain ratio of patients with repair was higher (i.e., muscle was less stiff) than that of the control during abduction 6 weeks post-surgery but recovered with postoperative duration; these authors also evaluated synergist muscles. It has been reported that there is no difference in the shear moduli of UT and MD muscles between repaired and contralateral unaffected shoulders during abduction throughout pre- and post-operative duration[23] and between the patient and control in MD muscle strain ratio 3 months after surgery.[43] Another study described the mechanical properties of the SSP muscle under passive conditions; however, other synergist muscles have not been studied in this regard. Itoigawa, et al. [22] showed that the shear modulus decreased in the first few months and then progressively improved 4 months after surgery. Our findings are consistent with these previous studies, confirming the validity of our task setting and ultrasound measurements.

Our comparison method considered the potential biases in the determination of muscle shear modulus. Previous studies indicated that muscle size and intramuscular fat influence the muscle shear modulus.[26-29] For instance, Dresner, et al. [27] demonstrated that the possibility of considerable variation in the individual slope of the shear modulus during isometric contraction was dependent upon muscle size and Pinel, et al. [28] showed that the age-related higher levels of intramuscular fat was associated with lower shear at the muscle length beyond its slack angle. Considering these facts, we included muscle thickness and echo intensity as covariates in the statistical model; nevertheless, our primary findings did not change. Therefore, although muscle size and composition may affect the shear modulus in some cases, they did not significantly affect our results.

Generally, muscle atrophy and fatty infiltration persist even after rotator cuff repair.[44; 45] Contrary to those of previous studies, our results showed that muscle thickness and echo intensity did not differ between repaired and control shoulders except for the significantly higher echo intensity of the MD muscle. There are some reasons explaining this discrepancy. As the tear size in our patients was limited to small and medium, there is a possibility that the extent of atrophy and fatty infiltration was minimal. A previous study reported that patients with partial-thickness tears did not demonstrate SSP muscle atrophy.[46] In terms of measurement technology, the ultrasound assessment could not detect muscle degenerations because the accuracy of ultrasound is slightly inferior to that of magnetic resonance imaging.[47; 48]

Additionally, the slight possibility of atrophy and fatty infiltration progress in the control shoulder could not be fully ignored. Regardless of these issues, our findings remain meaningful.

In interpreting our findings, the following should be noted. First, the intra-observer reliability of the elastography measurement is expected to be overestimated because using three consecutive images obtained by single probe positioning for the ICC calculation would make the inherent variability small among the images. Second, the present study design is not ideal because the cross-sectional design cannot identify time-dependent changes in compensation strategy. To comprehensively understand the compensation strategy, a prospective study throughout the different stages of rotator cuff tear and repair is essential. Third, whether the compensation strategy persists across various shoulder motions remains unknown because this study only focused on a single measurement posture and previous studies have demonstrated that depending upon the shoulder angle, the shear moduli of shoulder muscles vary during isometric contraction.[31; 49] Finally, a rule of compensation strategy and its individual difference could not be referred to as we did not conduct a thorough investigation that all possible muscles were evaluated. However, this study could at least demonstrate that the compensation strategy of shoulder abductors is not stereotypical.

In conclusion, this study identified the compensation strategy of shoulder abductors by examining synergist muscle response to muscle force deficit in the supraspinatus muscle in patients with small to medium rotator cuff repair. We observed no complementary relationship between the SSP and synergist muscles at the population level. Instead, we noted that the specific muscles acting to compensate for the SSP muscle varied among patients at an individual level. Our findings suggest that the compensation strategy for SSP muscle force deficit is non-stereotypical and varies among patients after small to medium rotator cuff repair. These results highlight the necessity of providing personalized rehabilitation programs following rotator cuff repair.

Acknowledgements

This work was supported by Grant-in-Aid for JSPS Fellow (18J12658).

Ethical Publication Statement

We confirm that we have read the Journal's position on issues involved in ethical publication and affirm that this report is consistent with those guidelines.

Disclosure of Conflicts of Interest

None of the authors have any conflict of interest to disclose.

References

1. Yamaguchi K, Tetro AM, Blam O, et al. 2001. Natural history of asymptomatic rotator cuff tears: a longitudinal analysis of asymptomatic tears detected sonographically. J Shoulder Elbow Surg 10:199-203.
2. Milgrom C, Schaffler M, Gilbert S, et al. 1995. Rotator-cuff changes in asymptomatic adults. The effect of age, hand dominance and gender. J Bone Joint Surg Br 77:296-298.
3. Yamamoto A, Takagishi K, Osawa T, et al. 2010. Prevalence and risk factors of a rotator cuff tear in the general population. J Shoulder Elbow Surg 19:116-120.
4. Hurley ET, Maye AB, Mullett H. 2019. Arthroscopic Rotator Cuff Repair: A Systematic Review of Overlapping Meta-Analyses. JBJS Rev 7:e1.
5. Thigpen CA, Shaffer MA, Gaunt BW, et al. 2016. The American Society of Shoulder and Elbow Therapists' consensus statement on rehabilitation following arthroscopic rotator cuff repair. J Shoulder Elbow Surg 25:521-535.
6. Edwards PK, Ebert JR, Littlewood C, et al. 2017. A Systematic Review of Electromyography Studies in Normal Shoulders to Inform Postoperative Rehabilitation Following Rotator Cuff Repair. J Orthop Sports Phys Ther 47:931-944.
7. van der Meijden OA, Westgard P, Chandler Z, et al. 2012. Rehabilitation after arthroscopic rotator cuff repair: current concepts review and evidence-based guidelines. Int J Sports Phys Ther 7:197-218.
8. Mehta S, Gimbel JA, Soslowsky LJ. 2003. Etiologic and pathogenetic factors for rotator cuff tendinopathy. Clin Sports Med 22:791-812.
9. Wolff AB, Sethi P, Sutton KM, et al. 2006. Partial-thickness rotator cuff tears. J Am Acad Orthop Surg 14:715-725.
10. de Witte PB, van der Zwaal P, van Arkel ER, et al. 2014. Pathologic deltoid activation in rotator cuff tear patients: normalization after cuff repair? Med Biol Eng Comput 52:241-249.
11. Fritz JM, Inawat RR, Slavens BA, et al. 2017. Assessment of Kinematics and Electromyography Following Arthroscopic Single-Tendon Rotator Cuff Repair. PM R 9:464-476.
12. Kelly BT, Williams RJ, Cordasco FA, et al. 2005. Differential patterns of muscle activation in patients with symptomatic and asymptomatic rotator cuff tears. J Shoulder Elbow Surg 14:165-171.
13. Dyrna F, Kumar NS, Obopilwe E, et al. 2018. Relationship Between Deltoid and Rotator Cuff Muscles During Dynamic Shoulder Abduction: A Biomechanical Study of Rotator Cuff Tear Progression. Am J Sports Med 46:1919-1926.
14. Oh JH, Jun BJ, McGarry MH, et al. 2011. Does a critical rotator cuff tear stage exist?: a biomechanical study of rotator cuff tear progression in human cadaver shoulders. J Bone Joint Surg Am 93:2100-2109.
15. Muench LN, Berthold DP, Otto A, et al. 2022. Increased Glenohumeral Joint Loads Due to a Supraspinatus Tear Can Be Reversed With Rotator Cuff Repair: A Biomechanical Investigation. Arthroscopy 38:1422-1432.
16. Khandare S, Arce RA, Vidt ME. 2022. Muscle compensation strategies to maintain glenohumeral joint stability with increased rotator cuff tear severity: A simulation study. J Electromyogr Kinesiol 62:102335.
17. Steenbrink F, Meskers CG, Nelissen RG, et al. 2010. The relation between increased deltoid activation and adductor muscle activation due to glenohumeral cuff tears. J Biomech 43:2049-2054.
18. Gennisson JL, Deffieux T, Mace E, et al. 2010. Viscoelastic and anisotropic mechanical properties of in vivo muscle tissue assessed by supersonic shear imaging. Ultrasound Med Biol 36:789-801.
19. Bouillard K, Nordez A, Hug F. 2011. Estimation of individual muscle force using elastography. PLoS One 6:e29261.
20. Ates F, Hug F, Bouillard K, et al. 2015. Muscle shear elastic modulus is linearly related to muscle torque over the entire range of isometric contraction intensity. J Electromyogr Kinesiol 25:703-708.

21. Baumer TG, Dischler J, Davis L, et al. 2018. Effects of age and pathology on shear wave speed of the human rotator cuff. J Orthop Res 36:282-288.
22. Itoigawa Y, Wada T, Kawasaki T, et al. 2020. Supraspinatus Muscle and Tendon Stiffness Changes After Arthroscopic Rotator Cuff Repair: A Shear Wave Elastography Assessment. J Orthop Res 38:219-227.
23. Sakaki Y, Taniguchi K, Sato F, et al. 2022. Time-course changes in active stiffness of the supraspinatus muscle after arthroscopic rotator cuff repair. J Med Ultrason (2001) 49:77-84.
24. Takagishi K, Makino K, Takahira N, et al. 1996. Ultrasonography for diagnosis of rotator cuff tear. Skeletal Radiol 25:221-224.
25. Ackland DC, Pak P, Richardson M, et al. 2008. Moment arms of the muscles crossing the anatomical shoulder. J Anat 213:383-390.
26. Koo TK, Hug F. 2015. Factors that influence muscle shear modulus during passive stretch. J Biomech 48:3539-3542.
27. Dresner MA, Rose GH, Rossman PJ, et al. 2001. Magnetic resonance elastography of skeletal muscle. J Magn Reson Imaging 13:269-276.
28. Pinel S, Kelp NY, Bugeja JM, et al. 2021. Quantity versus quality: Age-related differences in muscle volume, intramuscular fat, and mechanical properties in the triceps surae. Exp Gerontol 156:111594.
29. Gilbert F, Klein D, Weng AM, et al. 2017. Supraspinatus muscle elasticity measured with real time shear wave ultrasound elastography correlates with MRI spectroscopic measured amount of fatty degeneration. BMC Musculoskelet Disord 18:549.
30. Baumer TG, Davis L, Dischler J, et al. 2017. Shear wave elastography of the supraspinatus muscle and tendon: Repeatability and preliminary findings. J Biomech 53:201-204.
31. Hoshikawa K, Yuri T, Mura N, et al. 2021. Coordination of the Sub-Regions of the Supraspinatus and Deltoid Muscles During Shoulder Scaption: a Shear Wave Elastography Study. Muscle, Ligaments and Tendons Journal 11:569-576.
32. Itoigawa Y, Maruyama Y, Kawasaki T, et al. 2018. Shear Wave Elastography Can Predict Passive Stiffness of Supraspinatus Musculotendinous Unit During Arthroscopic Rotator Cuff Repair for Presurgical Planning. Arthroscopy 34:2276-2284.
33. Yuri T, Kobayashi H, Takano Y, et al. 2019. Capsular attachment of the subregions of rotator cuff muscles. Surg Radiol Anat 41:1351-1359.
34. Lacourpaille L, Hug F, Bouillard K, et al. 2012. Supersonic shear imaging provides a reliable measurement of resting muscle shear elastic modulus. Physiol Meas 33:N19-28.
35. Young HJ, Jenkins NT, Zhao Q, et al. 2015. Measurement of intramuscular fat by muscle echo intensity. Muscle Nerve 52:963-971.
36. Watanabe Y, Ikenaga M, Yoshimura E, et al. 2018. Association between echo intensity and attenuation of skeletal muscle in young and older adults: a comparison between ultrasonography and computed tomography. Clin Interv Aging 13:1871-1878.
37. Naruse M, Trappe S, Trappe TA. 2022. Human skeletal muscle size with ultrasound imaging: a comprehensive review. J Appl Physiol (1985) 132:1267-1279.
38. Stock MS, Thompson BJ. 2021. Echo intensity as an indicator of skeletal muscle quality: applications, methodology, and future directions. Eur J Appl Physiol 121:369-380.
39. Crowninshield RD, Brand RA. 1981. A physiologically based criterion of muscle force prediction in locomotion. J Biomech 14:793-801.
40. Langenderfer J, Jerabek SA, Thangamani VB, et al. 2004. Musculoskeletal parameters of muscles crossing the shoulder and elbow and the effect of sarcomere length sample size on estimation of optimal muscle length. Clin Biomech (Bristol, Avon) 19:664-670.
41. de Rugy A, Loeb GE, Carroll TJ. 2012. Muscle coordination is habitual rather than optimal. J Neurosci 32:7384-7391.
42. Hodges PW, Coppieters MW, MacDonald D, et al. 2013. New insight into motor adaptation to pain revealed by a combination of modelling and empirical approaches. Eur J Pain 17:1138-1146.
43. Ishikawa H, Muraki T, Morise S, et al. 2021. Changes in shoulder muscle activities and glenohumeral motion after rotator cuff repair: an assessment using ultrasound real-time tissue elastography. J Shoulder Elbow Surg 30:2577-2586.

44. Gladstone JN, Bishop JY, Lo IK, et al. 2007. Fatty infiltration and atrophy of the rotator cuff do not improve after rotator cuff repair and correlate with poor functional outcome. Am J Sports Med 35:719-728.
45. Deniz G, Kose O, Tugay A, et al. 2014. Fatty degeneration and atrophy of the rotator cuff muscles after arthroscopic repair: does it improve, halt or deteriorate? Arch Orthop Trauma Surg 134:985-990.
46. Maman E, Harris C, White L, et al. 2009. Outcome of nonoperative treatment of symptomatic rotator cuff tears monitored by magnetic resonance imaging. J Bone Joint Surg Am 91:1898-1906.
47. Strobel K, Hodler J, Meyer DC, et al. 2005. Fatty atrophy of supraspinatus and infraspinatus muscles: accuracy of US. Radiology 237:584-589.
48. Wall LB, Teefey SA, Middleton WD, et al. 2012. Diagnostic performance and reliability of ultrasonography for fatty degeneration of the rotator cuff muscles. J Bone Joint Surg Am 94:e83.
49. Hoshikawa K, Yuri T, Giambini H, et al. 2022. The functional role of the supraspinatus and infraspinatus muscle subregions during forward flexion: a shear wave elastography study. JSES Int 6:849-854.

Figure 1. Ultrasound measurement and image processing. (A) Passive abduction. A physiotherapist (S.N. or K.K.) supported the arm of the patient at 30° of shoulder abduction with a fully extended elbow joint, natural wrist posture, and thumb pointing upward in a fully relaxed manner. In cases where the patients were evaluated as not relaxed by assessment of physiotherapist and identification of muscle fiber motion via ultrasound, the patients were instructed not to activate muscles as much as possible. The yellow dash lines in the image delineate the muscle boundary. The colormap within the region of interest represents that red and blue are high and low values of Young's modulus, respectively. (B) Active abduction. The patients voluntarily abducted their shoulder at 30° and maintained this posture with other joints in the same position as the passive abduction. In the case where compensatory movements such as excessive lateral flexion of the trunk and scapular elevation were identified, we instructed them to correct the posture. The shoulder joint angle was secured using a goniometer. (C) Natural posture. Shoulder abduction at approximately 0°, full elbow extension, and neutral wrist and hand postures. We instructed them to be relaxed as much as possible. The white arrow line represents muscle thickness, and the white rectangular box represents the region of interest for echo intensity analysis. SSP, supraspinatus muscle; UT, upper trapezius muscle; ISP, infraspinatus muscle; MD, middle deltoid muscle.

Figure 2. Shear modulus of repaired and control shoulders during abduction tasks. (A) Supraspinatus, (B) upper trapezius, (C) infraspinatus, and (D) middle deltoid muscles are displayed. Red and gray colors represent repaired and control shoulders, respectively. Circle and triangle plots represent passive and active abductions, respectively. The filled plot and error bar express the mean and standard deviation, respectively. Empty plots indicate data from individual patients. Asterisk and dagger indicate significant main effect of contraction condition ($p < 0.001$) and shoulder side ($p < 0.05$), respectively. Details regarding the statistical values of ANOVAs are listed in Table 4. SSP, supraspinatus muscle; UT, upper trapezius muscle; ISP, infraspinatus muscle; MD, middle deltoid muscle.

Figure 3. Linear regression analysis between the supraspinatus and other synergist muscles. The active shear moduli of the supraspinatus and each synergist muscle are specified as independent and dependent variables. There was no significant association between the supraspinatus and (A) upper trapezius, (B) infraspinatus, and (C) middle deltoid muscles. n.s., not statistically significant; SSP, supraspinatus muscle; UT, upper trapezius muscle; ISP, infraspinatus muscle; MD, middle deltoid muscle.

Figure 4. Individual analysis for the compensation strategy. (A) The ratio of shear modulus between repaired and control shoulders of each patient during active abduction is displayed as a bicolor table. In the table, rows and columns represent each patient (from 1–15) and muscle (SSP, UT, ISP, and MD), respectively. Red and blue cells represent the high and low shear moduli, respectively, of the repaired shoulder relative to that of the control shoulder. In other words, the ratio of one means that the shear active moduli are equal between repaired and control shoulders. Patients #1, 2, 3, 4, 7, 8, 10, 14, and 15 underwent rotator cuff repair on their dominant limb. (B) The ratio of shear modulus is expressed as the rank-order table. Rows and columns are the same as in panel A. Fourth ordered cell filled in red color represents the highest ratio of shear modulus among all muscles. (C) Shoulder pain (top), Western Ontario Rotator Cuff Index (middle), and postoperative day (bottom) are presented in subgroups of the upper trapezius, infraspinatus, and middle deltoid muscles. The dot represents the data from each

patient. SSP, supraspinatus muscle; UT, upper trapezius muscle; ISP, infraspinatus muscle; MD, middle deltoid muscle. WORC, Western Ontario Rotator Cuff Index; POD, postoperative day.

Table 1. Shoulder characteristics, function, and symptoms

	Repaired	Control	Statistic value
ROM, flexion (°)	138 ± 19	159 ± 12 *	$p = 0.001$, $r = 0.85$
ROM, abduction (°)	139 ± 22	165 ± 10 *	$p < 0.001$, $r = 0.93$
ROM, external rotation (°)	42 ± 24	68 ± 13 *	$p < 0.001$, $d = 1.29$
Dominant limb (%)	60	40	—
Postoperative day (days)	112 ± 62	—	—
Tear type (n)	partial-thickness 2, full-thickness 13	—	—
Tear size (n)	small 10, medium 5	—	—
WORC (points)	902 ± 326	—	—
Pain (mm)	32 ± 28	—	—

Data are shown as mean ± SD. The *p*- and Cohen's d or r values are presented as statistical values and their effect sizes, respectively. The asterisk represents a significant difference between repaired and control shoulders. Shoulder pain was evaluated on a visual analog scale using the first item in the WORC physical symptoms. SSP, supraspinatus muscle; ISP, infraspinatus muscle; ROM, range of motion, WORC, Western Ontario Rotator Cuff Index.

Table 2. Intra-observer reliability for elastography and B-mode measurements

ICC$_{1,k}$ (95%CI)					
Contraction condition	Shoulder side	Elastography measurement			
		SSP	UT	ISP	MD
Passive condition	Repair	0.95 (0.88 – 0.98)	0.99 (0.99 – 0.99)	0.91 (0.78 – 0.97)	0.99 (0.97 – 0.99)
	Control	0.95 (0.88 – 0.98)	0.99 (0.98 – 0.99)	0.95 (0.88 – 0.98)	0.99 (0.98 – 0.99)
Active condition	Repair	0.86 (0.67 – 0.95)	0.99 (0.98 – 0.99)	0.97 (0.94 – 0.99)	0.94 (0.87 – 0.98)
	Control	0.97 (0.94 – 0.99)	0.99 (0.98 – 0.99)	0.98 (0.94 – 0.99)	0.95 (0.88 – 0.98)
	Shoulder side	B-mode measurement			
		SSP	UT	ISP	MD
Muscle thickness	Repair	0.98 (0.96 – 0.99)	0.85 (0.59 – 0.95)	0.99 (0.97 – 0.99)	0.99 (0.98 – 0.99)
	Control	0.99 (0.99 – 0.99)	0.99 (0.97 – 0.99)	0.99 (0.98 – 0.99)	0.82 (0.47 – 0.94)
Echo intensity	Repair	0.99 (0.98 – 0.99)	0.99 (0.98 – 0.99)	0.99 (0.97 – 0.99)	0.99 (0.98 – 0.99)
	Control	0.99 (0.99 – 0.99)	0.99 (0.98 – 0.99)	0.99 (0.99 – 0.99)	0.99 (0.99 – 0.99)

Data represent ICC$_{1,k}$ and its 95% confidence interval. The ICC$_{1,k}$ was calculated using the model for case 1, where k is the number of repetitive measurements. These ICCs show the reliabilities of two and three repetitive measurements for elastography and B-mode measurements, respectively. ICC, intraclass correlation coefficient; 95% CI, 95% confidence interval; SSP, supraspinatus muscle; UT, upper trapezius muscle; ISP, infraspinatus muscle; middle deltoid muscle.

Table 3. Comparison of muscle thickness and echo intensity between repaired and control shoulders

		Muscle thickness (mm)	
Muscle	Repaired	Control	Statistic value
SSP	18.0 ± 2.8	16.6 ± 3.2	p = 0.186, d = 0.45
UT	13.9 ± 2.9	13.3 ± 2.8	p = 0.347, d = 0.20
ISP	15.1 ± 3.5	15.2 ± 3.6	p = 0.921, d = 0.03
MD	19.6 ± 4.7	20.0 ± 3.6	p = 1.000, r < 0.01
		Echo intensity (a.u.)	
Muscle	Repaired	Control	Statistic value
SSP	57.9 ± 11.9	53.5 ± 16.0	p = 0.263, d = 0.31
UT	71.4 ± 16.9	68.2 ± 15.9	p = 0.116, d = 0.19
ISP	61.7 ± 20.2	61.8 ± 19.0	p = 0.981, d < 0.01
MD	69.7 ± 16.9	64.0 ± 13.9	p = 0.044, d = 0.36 *

Data are shown as mean ± SD. The *p*- and Cohen's d or r values are presented as statistical values and their effect sizes, respectively. The asterisk represents a significant difference between repaired and control shoulders. SSP, supraspinatus muscle; UT, upper trapezius muscle; ISP, infraspinatus muscle; MD, middle deltoid muscle.

Table 4. Statistical values of ANOVA for the LME model for each muscle

Muscle	ANOVA for LME model								
	Interaction			Main effect					
				Shoulder side			Contraction condition		
	F	p	η^2_p	F	p	η^2_p	F	p	η^2_p
SSP	1.67	0.206	0.03	9.54	0.005	0.15	75.00	< 0.001	0.59
UT	< 0.01	0.983	< 0.01	0.92	0.345	0.02	60.45	< 0.001	0.63
ISP	0.04	0.837	< 0.01	0.12	0.736	< 0.01	31.63	< 0.001	0.40
MD	3.07	0.090	0.06	1.27	0.270	0.02	112.55	< 0.001	0.69
ALL		-		0.27	0.601	< 0.01		-	

Muscle	ANOVA for LME model with covariates								
	Interaction			main effect					
				Shoulder side			Contraction condition		
	F	p	η^2_p	F	p	η^2_p	F	p	η^2_p
SSP	2.09	0.154	0.04	13.95	< 0.001	0.21	93.90	< 0.001	0.63
UT	< 0.01	0.983	< 0.01	1.65	0.210	0.05	60.45	< 0.001	0.64
ISP	0.04	0.837	< 0.01	0.11	0.748	< 0.01	31.63	< 0.001	0.41
MD	3.07	0.091	0.05	1.11	0.302	0.02	112.55	< 0.001	0.70
ALL		-		1.11	0.293	< 0.01		-	

The F- and p-values and η^2_p are presented as statistical values and their effect sizes, respectively. ANOVA, analysis of variance; LME model, linear mixed effect model; SSP, supraspinatus muscle; UT, upper trapezius muscle; ISP, infraspinatus muscle; MD, middle deltoid muscle, ALL; all muscles.

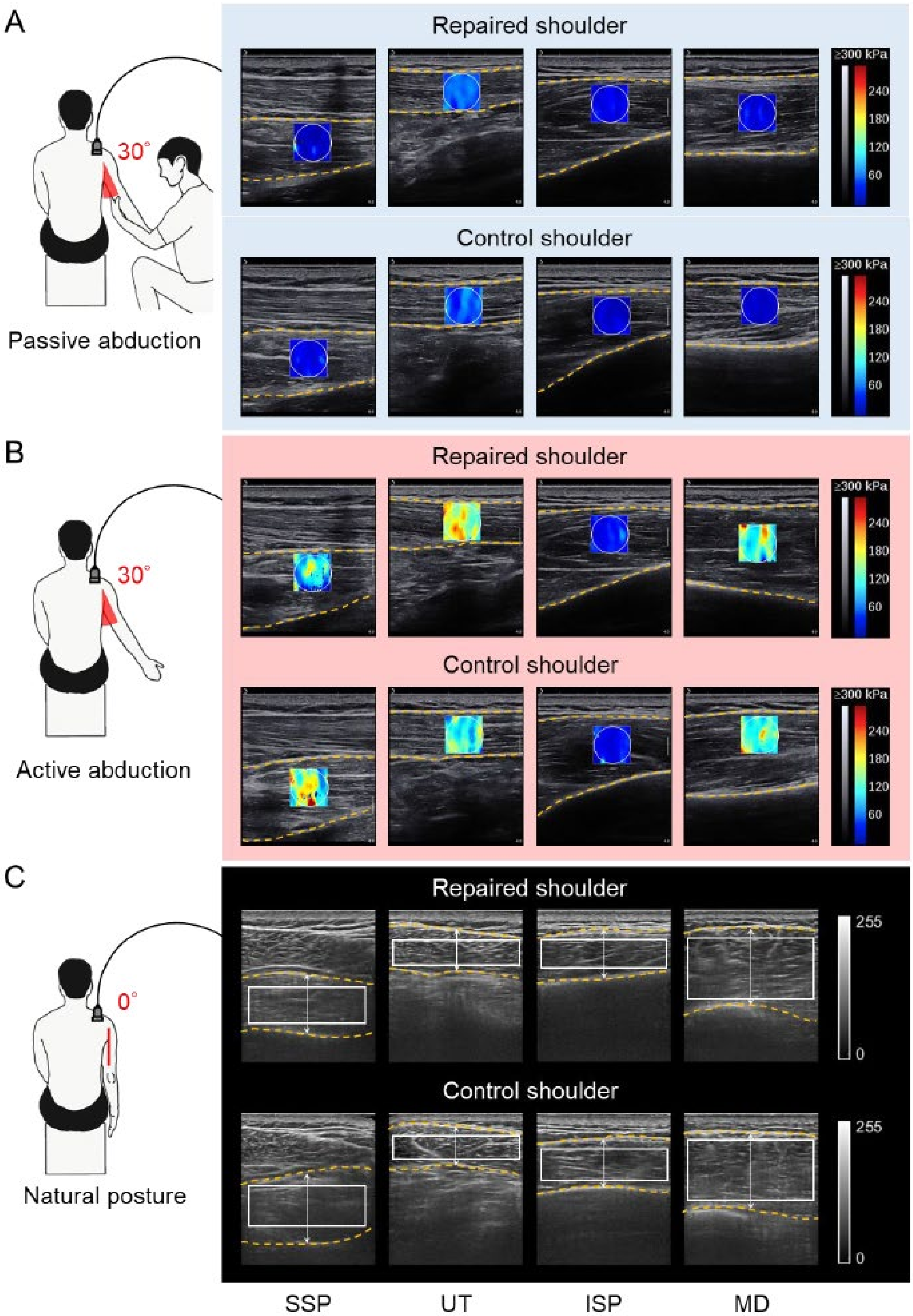
A
Repaired shoulder
≥300 kPa
240
180
120
60
30°
Passive abduction
Control shoulder
B
Active abduction
C
0°
Natural posture
255
0
SSP
UT
ISP
MD

Figure 1

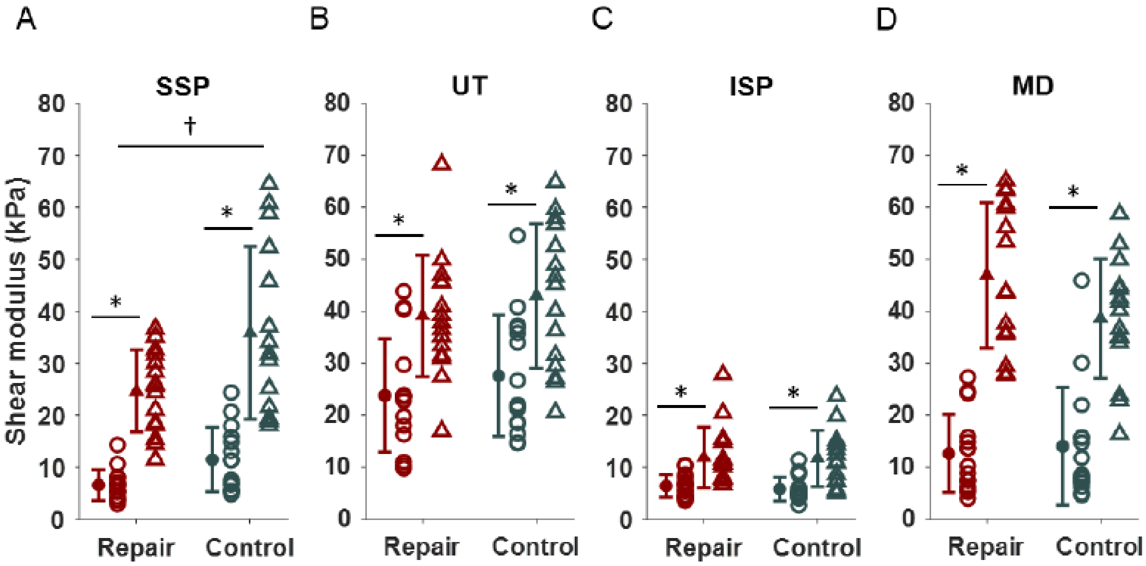
A
B
C
D
SSP
UT
ISP
MD
Shear modulus (kPa)
0
10
20
30
40
50
60
70
80
Repair
Control
*
†

Figure 2

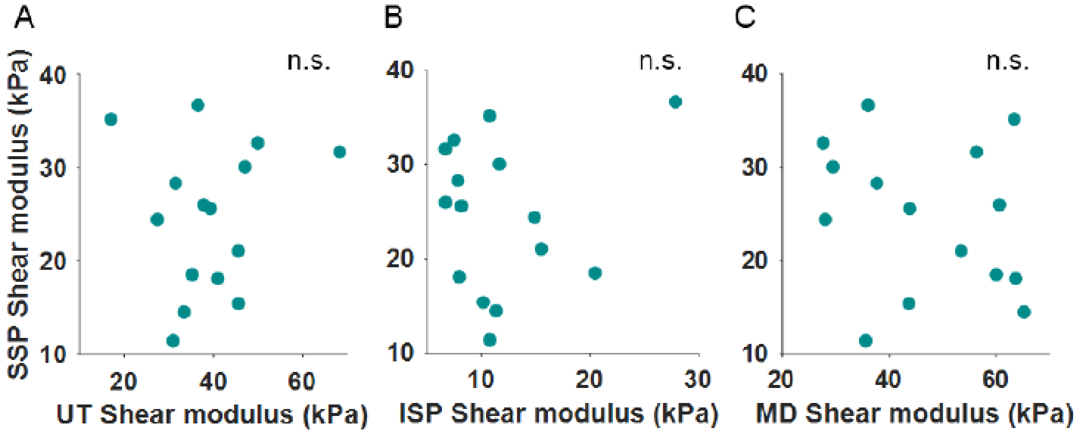
A
B
C
n.s.
n.s.
n.s.
SSP Shear modulus (kPa)
UT Shear modulus (kPa)
ISP Shear modulus (kPa)
MD Shear modulus (kPa)

Figure 3

A

Ratio of shear modulus

Patient	SSP	UT	ISP	MD
1	0.83	1.19	0.58	0.64
2	0.61	1.2	0.92	2.36
3	1.02	1.45	0.75	0.88
4	0.85	1.54	0.67	2.66
5	1.15	0.61	5.59	1.06
6	0.93	1.3	1.47	1.81
7	0.4	1.04	0.46	1.14
8	0.54	0.77	0.6	0.65
9	0.6	0.83	1.89	1.43
10	0.57	0.93	1.78	1.33
11	0.75	0.83	1.02	1.56
12	0.86	0.67	2.73	1.63
13	0.61	0.66	0.54	0.79
14	0.53	0.47	1.03	0.8
15	0.98	1.04	0.49	1.29

B

Order of ratio

Patient	SSP	UT	ISP	MD
1	3	4	1	2
2	1	3	2	4
3	3	4	1	2
4	2	3	1	4
5	3	1	4	2
6	1	2	3	4
7	1	3	2	4
8	1	4	2	3
9	1	2	4	3
10	1	2	4	3
11	1	2	3	4
12	2	1	4	3
13	2	3	1	4
14	2	1	4	3
15	2	3	1	4

C

Subgroup characteristics

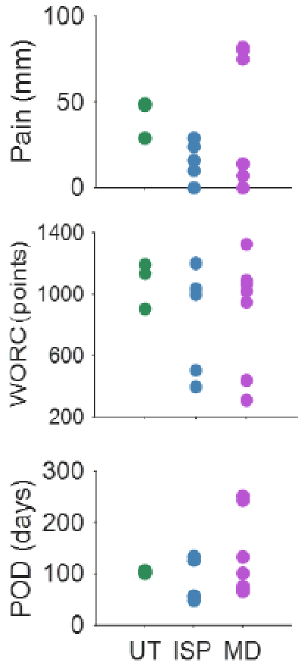

Figure 4